HHS Public Access

Author manuscript

Neuroscience. Author manuscript; available in PMC 2024 July 01.

Published in final edited form as:

Neuroscience. 2023 July 01; 522: 42–56. doi:10.1016/j.neuroscience.2023.04.020.

Progressive Dysregulation of Tau Phosphorylation in an Animal Model of Temporal Lobe Epilepsy

FA Concepcion[*],

NA Ekstrom[*],

MN Khan,

OO Estes,

NP Poolos[#]

Department of Neurology and Regional Epilepsy Center, University of Washington, Seattle, WA

Abstract

Tau is an intracellular protein known to undergo hyperphosphorylation and subsequent neuro-toxic aggregation in Alzheimer's disease (AD). Here, tau expression and phosphorylation at three canonical loci known to be hyperphosphorylated in AD (S202/T205, T181, and T231) were studied in the rat pilocarpine status epilepticus (SE) model of temporal lobe epilepsy (TLE). We measured tau expression at two time points of chronic epilepsy: two months and four months post-SE. Both time points parallel human TLE of at least several years. In the whole hippocampal formation at two months post-SE, we observed modestly reduced total tau levels compared to naïve controls, but no significant reduction of S202/T205 phosphorylation levels. In the whole hippocampal formation from four month post-SE rats, total tau expression had reverted to normal, but there was a significant reduction in S202/T205 tau phosphorylation levels that was also seen in CA1 and CA3. No change in phosphorylation was seen at the T181 and T231 tau loci. In somatosensory cortex, outside of the seizure onset zone, no changes in tau expression or phosphorylation were seen at the later time point. We conclude that total tau expression and phosphorylation in an animal model of TLE studied do not show hyperphosphorylation at the three AD canonical tau loci. Instead, the S202/T205 locus showed progressive dephosphorylation. This suggests that changes in tau expression may play a different role in epilepsy than in AD. Further study is needed to understand how these changes in tau may impact neuronal excitability in chronic epilepsy.

Introduction

Tau is an intracellular protein that under normal conditions regulates neuronal microtubule structure dynamics, but in the setting of Alzheimer's disease (AD) plays a pathological role.

[#]Corresponding author: Nicholas P. Poolos, MD, PhD, Department of Neurology and Regional Epilepsy Center, Box 359745, 325 9th Ave, Seattle, WA 98104, npoolos@uw.edu, 206-897-5423.

[*]These authors contributed equally

During the development of AD, increased phosphorylation of tau is the primary molecular mechanism that underlies its pathogenicity. Under normal physiological conditions, tau is phosphorylated at low levels, two moles of phosphate per mole of tau. In AD, tau phosphorylation rises four-fold to eight moles per mole of tau (Wang & Mandelkow, 2016). This “hyperphosphorylation” causes tau to dissociate from microtubules, impairing microtubule function. The dissociated tau can then form oligomers and further coalesce into paired helical filaments and extracellular neurofibrillary tangles. In AD, 17 separate amino acid loci or “phosphosites” have been observed to be hyperphosphorylated compared to normal conditions (Li & Götz, 2017). Several of these are used as representative loci in the diagnosis of AD. Phosphospecific antibodies (Abs) that recognize tau phosphosites only when phosphorylated have become standard reagents for detection of tauopathy. Examples include the AT8 Ab which recognizes dual phosphorylation at the human S202/T205 tau locus; AT270 Ab which recognizes phosphorylation at the T181 site; and 1H6L6 Ab which is specific for T231. The AT8 Ab is the standard reagent used in Braak staging of AD progression in post-mortem brain tissue (Wang et al., 2013).

Tau expression may be altered in human temporal lobe epilepsy (TLE) as well. An early study using immunohistochemical (IHC) methods in autopsy tissue found an overall increase in Braak staging throughout the brains of people with epilepsy of all types, but in TLE there was a loss of AT8 staining in the hippocampus at the site of presumed seizure onset (the side showing mesial temporal sclerosis) compared to the contralateral side (Thom et al., 2011). A similar study using resected tissue at time of surgery for patients with drug-resistant TLE found increased AT8 staining in a subpial distribution (but little in the hippocampus itself) with the overall increase in AT8 expression correlated with cognitive decline (Tai et al., 2016). A study that used western blotting to evaluate tau expression in temporal lobe resection tissue found an increase in total tau expression compared to autopsy controls; this study also found an increase in AT8 expression that was comparable to the increase in total tau expression, implying no change in the fractional phosphorylation level of tau at this phosphosite (Gourmaud et al., 2020). More recent studies of patients who underwent temporal lobe resection found either only a low incidence of neurons staining for phosphorylated tau using AT8 Ab (Silva et al., 2021), or some staining for phosphorylated tau but no correlation with cognitive decline (Aroor et al, in press). Other studies have found AT8 staining in both young epilepsy patients with cortical resections and older patients diagnosed with focal cortical dysplasia (FCD), which may reflect differing pathologies in children with refractory epilepsy or adults with FCD (Sen et al., 2007; Smith et al., 2019). Finally, measurements of tau expression from cerebrospinal fluid (CSF) in patients with epilepsy have found either lowered total tau but increased fractional phosphorylation at the T181 tau locus in TLE patients compared to controls (Mo et al., 2019), or no significant change in total tau in a cohort of mixed epilepsy syndromes (Palmio et al., 2009). In summary, it is unclear in human epilepsy whether tau expression and phosphorylation follow the same pattern as in AD. Limitations in some of these studies include reliance on IHC, which provides only a qualitative measure to assess tau expression; the use of autopsy tissue which may not preserve the phosphorylation state of tau; and the omission of total tau analysis that is necessary to place changes in phosphorylated tau into context.

Studies in animal models of epilepsy however have uncovered an important biological role for tau. Creation of double transgenic mouse models of epilepsy, such as the *kcna1*$^{-/-}$ or *scna1*$^{-/-}$ crossed with tau deletion (*mapt*$^{-/-}$), showed that the seizures in these models are virtually abolished when tau is deleted (Holth et al., 2013; Gheyara et al., 2014; Shao et al., 2022). (Another study using the SCN2A model of epilepsy found no improvement in survival in mice with tau deletion, although seizures themselves were not measured (Chen et al., 2018)). This remarkable effect of tau loss of function on seizures is not limited to genetic models of epilepsy: downregulation of tau expression via antisense techniques prevents chemically-induced seizures in wildtype rodents (DeVos et al., 2013) or spontaneous seizures in SCN1A mutant mice (Shao et al., 2022). Hyperphosphorylation of tau may reduce seizures by reducing pyramidal neuron excitability through an action on axon morphology dependent on microtubule stability (Hatch et al., 2017). These studies suggest that tau plays a permissive role in the mechanism of seizure generation.

The above studies explored whether modulation of tau expression could affect seizure generation in animal models of epilepsy. Only a few studies have examined whether changes in tau expression or phosphorylation occur in animal models of acquired epilepsy as are observed in humans with epilepsy (Alves et al., 2019; Canet et al., 2022). In this study we sought to understand how both total tau expression and phosphorylation at three canonical loci known to be pathologically hyperphosphorylated in AD may change in a well-validated animal model of TLE. We investigated tau expression at two different time points in chronic epilepsy comparable to the course of TLE in humans who have experienced seizures for years. We found that total tau expression was initially reduced in the earlier stage of chronic epilepsy, two months post-SE, but had normalized at a later stage, four months post-SE, even though spontaneous seizure frequency remained high. However, phosphorylation at the S202/T205 locus was progressively decreased during the course of chronic epilepsy, becoming dephosphorylated by ~50% compared to age-matched controls. No changes were seen at the T181 and T231 tau loci at the later time point, nor in the somatosensory cortex, a region outside the hippocampal epileptogenic zone. These findings suggest that tau expression and phosphorylation in an animal model of TLE do not follow the pattern seen in human AD, but may reflect physiological responses that are specific to the chronically epileptic state.

Experimental Procedures

Pilocarpine-induced status epilepticus (SE)

Experimental animals were generated using the pilocarpine protocol as previously described (Jung et al., 2007). The University of Washington Institutional Animal Care and Use Committee approved all animal procedures. In brief, 6-week-old male Sprague Dawley rats underwent induction of SE with pilocarpine hydrochloride (385 mg/kg intraperitoneal [i.p.]) after pretreatment with scopolamine methyl nitrate (1 mg/kg i.p.). After 60 min of convulsive SE, seizures were terminated with repeated doses of phenobarbital (15 mg/kg i.p.) every 30-45 min until cessation of convulsive motor activity. Rats were sacrificed at two time points, two months post-SE and four months post-SE. At sacrifice, these rats were exposed to isoflurane (5%) and injected with ketamine/xylazine anesthesia (87/13 mg/kg

i.p.). Age-matched, singly housed naïve rats were used as controls and were sacrificed at the same time points and conditions described above. After brain slicing using previously described procedures (Williams et al., 2015), rat brain slices were frozen and stored at −80 °C.

Western analyses

Quantification of protein expression from hippocampal tissue via western blotting was performed as previously described (Williams et al., 2015; Tai et al., 2017; Parikh et al., 2020; Concepcion et al., 2021). In this study, we examined the whole hippocampal formation (CA1 hippocampus, CA3 hippocampus, dentate gyrus, subiculum, and entorhinal cortex), as well as separate CA1 and CA3 hippocampus, and somatosensory cortex. Each of these regions was microdissected from frozen rat brain slices at −20 °C, pooled, and homogenized in the following buffer: 50 mM Tris, 5 mM ethylenediaminetetraacetic acid (EDTA), 50 mM NaCl, 1 mM sodium orthovanadate, 10 mM ethylene glycol-bis(2-aminoethylether)-N,N,N’,N’-tetraacetic acid (EGTA), 2 mM sodium pyrophosphate, 4 mM para-nitrophenyl phosphate, 4 μg/ml aprotinin, 20 μg/ml leupeptin, 1 mM phenylmethylsulfonyl fluoride, and 1 % Triton X-100 (Roberson et al., 1999). After centrifuging at 20,800 x g at 4 °C for 15 min, the supernatant was transferred to a clean tube. Protein concentrations were determined by a bicinchoninic acid (BCA) assay (Pierce, ThermoFisher Scientific, Waltham, MA). Samples then were mixed with an equal volume of 2X Laemmli buffer (5% β-mercaptoethanol).

To generate phosphatase-treated homogenates of the whole hippocampal formation, similar steps as described above for microdissection and homogenization were used. The microdissected whole hippocampal formation was homogenized in modified buffer with the following recipe: 50 mM Tris, 1 mM EDTA, 50 mM NaCl, 1 mM EGTA, 4 μg/ml aprotinin, 20 μg/ml leupeptin, 1 mM phenylmethylsulfonyl fluoride, and 1% Triton X-100. The steps for centrifuging and extracting supernatant were the same as previously mentioned. After the addition of NEBuffer (final concentration 1X), $MnCl_2$ (final concentration 1 mM), and lambda protein phosphatase (New England Biolabs, Ipswich, MA; # P0753S), the homogenates were incubated at 30 °C for 30 minutes. Thereafter, samples were then processed in the same manner as non-phosphatase treated samples.

Each prepared sample was boiled and loaded in multiple lanes with three different amounts to ensure signal detection occurred within a linear range (Jung et al., 2010; Tai et al., 2017; Parikh et al., 2020; Concepcion et al., 2021). Each 4–15% polyacrylamide gel (Bio-Rad Laboratories, Hercules, CA) contained one experimental sample and one age-matched control sample to allow for comparisons within the same blot. After transferring proteins to a nitrocellulose membrane, we performed western blotting. All antibodies (Abs) were diluted in blocking buffer composed of 5% milk with 1X tris-buffered saline with 0.1% Tween-20 (TBST). The following pairings of Abs were used: AT8 Ab, (1:250; ThermoFisher Scientific; #ENMN1020) with α-mouse IgG1-IRDye® 800CW (1:5000; Li-Cor Biosciences, Lincoln, NE; #926-32210). (Of note, both the human serine 202 and human threonine 205 residues (S202/T205) must be phosphorylated to be recognized by the AT8 monoclonal Ab [Figure 1B]).

AT270 Ab (1:1000; ThermoFisher Scientific; ENMN1050) with either α-mouse IgG (H+L)-Dylight-680 (1:8000; ThermoFisher Scientific; # PI35519) or α-mouse IgG (H+L)-Dylight-800 (1:8000; ThermoFisher Scientific; # SA5-10176). (Of note, threonine 181 [T181] must be phosphorylated to be recognized by the AT270 monoclonal Ab [Figure 1B]). 1H6L6 Ab (1:700; ThermoFisher Scientific; PI701056) with either α-rabbit IgG (H+L)-Dylight 800 (1:5000; ThermoFisher Scientific; #PISA5-10036) or α-rabbit IgG (H+L)-IRDye® 680RD (1:5000; Li-Cor Biosciences; #926-68071). (Of note, threonine 231 [T231] must be phosphorylated to be recognized by the 1H6L6 monoclonal Ab [Figure 1B]). Tau 5 Ab (1:1000; Abcam, Waltham, MA; #ab80579) with α-mouse IgG (H+L)-Dylight-680 (1:8000; ThermoFisher Scientific; # PI35519); α-4R tau Ab (1:1000; Abcam; #ab218314) with either α-rabbit IgG (H+L)-Dylight 800 (1:5000; ThermoFisher Scientific; #PISA5-10036) or α-rabbit IgG (H+L)-IRDye® 680RD (1:5000; Li-Cor Biosciences; #926-68071); α-3R tau Ab (1:500; Millipore-Sigma, St. Louis, MO; #05-503) with α-mouse IgG-light chain (1:1000; Millipore-Sigma; #AP200) coupled with IRDye® 800CW (Li-Cor Biosciences coupling kit; #928-38040).

Detection and analyses of signals from fluorescent secondary antibodies were achieved with the Odyssey CLx Image Studio software (Li-Cor Biosciences). Protein level measurements were accomplished as previously described (Jung et al., 2010). Briefly, we loaded multiple lanes with three different protein amounts for each rat homogenate sample, and band intensity for each lane was quantified. A linear function was fit for band intensity vs. protein amount (including the origin), and the slope of the line (m) estimated. A minimum coefficient of determination (R^2) value of 0.9 was used as criterion for accepting data from the experiment. Comparisons between the test and control conditions were calculated as the ratio of the slopes (m_{test}/m_{ctrl}) for samples loaded within the same blot. Statistics are reported as means ± SEM. With $\alpha = 0.05$, significance was determined by two-tailed t-tests for data sets with Gaussian distribution or by non-parametric (Wilcoxon) testing for data sets not having a Gaussian distribution. Verification of protein loading was achieved by staining a subset of gels with REVERT™ Total Protein Stain (Li-Cor Biosciences; cat# 103051-156) and comparing the ratio of total protein between test and control conditions. The average test:control ratio per gel was 98.3 ± 1.7% ($n = 22$, $p > 0.05$), showing excellent consistency in gel loading.

Immunohistochemistry

Four month post-SE rats and their age-matched naïve controls were perfused with 200 mL of 1X phosphate buffered saline (PBS) and then 200 mL of 4% paraformaldehyde in 1X PBS. The brain was extracted and then incubated in 4% paraformaldehyde in 1X PBS for three hours at room temperature, then in 15% sucrose overnight followed by 30% sucrose for 3-5 days. After infiltration, the brains were flash frozen in Tissue-Tek O.C.T. Compound (Sakura Finetek, Torrance, CA) using liquid nitrogen. Oblique axial sections were taken at 10 μm using a cryostat (CM1850, Leica Biosystems, Wetzlar, Germany). Sections were then mounted on slides and stored at −80 °C. After thawing, antigen retrieval was performed by submerging the slices in sodium citrate (pH=6) at 90 °C for 20 minutes. Slices were washed with 1X PBS with 0.05% Tween-20 detergent (PBS-T) and were incubated in blocking buffer (2% normal goat serum, 2% bovine serum albumin, 1X PBS with 0.25% Tween-20) at

room temperature for one hour. The slices then were incubated with primary AT8 Ab (1:50 in blocking buffer) overnight at 4 °C. Slices were then washed with blocking buffer and then stained with a secondary α-mouse IgG1-biotin-xx, cross-adsorbed (1:267 in blocking buffer; ThermoFisher Scientific; # A10519) followed by an incubation with a streptavidin conjugated to Alexa 488 (1:267 in blocking buffer; Fisher Scientific; # S323354). Slices were fixed with 4% paraformaldehyde for 5 minutes and then incubated with DAPI (4', 6-diamidino-2-phenylindole; VWR, Radnor, PA, cat# 76482-854) for 5 minutes. Slices were mounted using Vectashield (Vector Laboratories, Newark, CA). Images were captured with a confocal microscope (Olympus FV 1000, Olympus Scientific Solutions Americas Corp., Tokyo, Japan). Post-capture images were created using ImageJ (Image Processing and Analysis in Java; NIH), and quantification of IHC was performed in ImageJ by drawing three boxes of equal area in an area of interest and then taking the average of the pixel density of all three boxes. Statistical parameters were similar to those described above.

Results

Accumulation and hyperphosphorylation of tau are widely known in Alzheimer's disease (AD) (Medeiros et al., 2011). Inspired by the extensive research of tau in AD and by the growing evidence for common biochemical pathways between AD and epilepsy (Gourmaud et al., 2020; Romoli et al., 2021), we aimed to understand whether changes in tau expression and phosphorylation also occur in chronic epilepsy. To achieve this end, we used the pilocarpine-induced status epilepticus (SE) rat model for human temporal lobe epilepsy (Curia et al., 2008), a well validated model with which we have extensive experience (Jung et al., 2007; Jung et al., 2010; Tai et al., 2017; Parikh et al., 2020; Concepcion et al., 2021). As in humans, tau in the rat central nervous system consists of six isoforms (Hanes et al., 2009) that are determined by alternative splicing of two N-terminal exons and the second repeat region within its microtubule binding domain (MBD, Figure 1A). The absence of the second repeat within the MBD generates the 3R tau isoforms (0N3R, 1N3R, 2N3R), and its presence generates the 4R tau isoforms (0N4R, 1N4R, 2N4R). Figure 1B shows the overlap of the human and rat tau protein sequences, demonstrating significant overlap between the two sequences, with the human tau sequences having a greater length than the rat sequences.

We investigated tau expression at two time points in chronic epilepsy, two months post-SE and four months post-SE (Figure 1C). These time points represent conditions when the animals are having frequent spontaneous seizures. We examined the whole hippocampal formation where seizures are known to originate in this model (Toyoda et al., 2013; Buckmaster et al., 2022), including the hippocampus proper (areas CA1, CA3 and dentate gyrus [*DG*]) plus the subiculum (*Sub*) and entorhinal cortex (*EC*), and separately studied just the CA1 and CA3 hippocampal regions. We also studied a non-epileptogenic region of the brain where seizures do not arise in this model, the somatosensory cortex (*SSC*), that served as a control (Figure 1D).

Characterization of tau isoforms by western blotting

We first analyzed total tau expression and dual phosphorylated S193/T196 tau, which is the rat homolog of human S202/T205 tau, in brain homogenates of naive rats at two

different ages, six weeks-old and 12 weeks-old, to determine which of the six isoforms were expressed in hippocampal tissue. We utilized two antibodies (Abs) to identify the tau isoforms consisting of either three or four repeated domains using anti-3R tau and anti-4R tau Abs. In six week-old rats (Figure 2A), 4R tau staining in raw homogenates (*upper panel)* showed tau migration between 50-72 kDa that consolidated into three distinct bands upon treatment with phosphatase [*(+)pptase lane*]. From lowest to highest molecular weight, by comparison to the human tau ladder, these bands in the treated lane are the 0N4R, 1N4R, and 2N4R isoforms. With 3R tau staining (*middle panel*), a doublet around 50 kDa in raw homogenate lanes coalesced into the lower band after phosphatase treatment. Therefore, this doublet is 0N3R tau, with phosphorylation responsible for generating the slightly higher molecular weight band. The other 3R tau isoforms, 1N3R and 2N3R, were not appreciably detected. Taken together, rat tau expression in raw homogenates consists of four measurable tau isoforms (2N4R, 1N4R, 0N4R, and 0N3R); the 1N3R and 2N3R isoforms are not readily detectable and contribute insignificantly to total tau protein staining. When compared to the human tau ladder that consists of six tau isoforms, all detected dephosphorylated rat tau isoforms migrated at slightly lower molecular weights than their corresponding human orthologs, since rat tau isoforms have fewer amino acid residues than their human counterparts. Moreover, as shown by the *yellow arrows* in a raw homogenate lane illustrating the presence of both 0N3R and 0N4R within the same band, different tau isoforms may co-migrate, making it difficult to discern individual tau isoforms. The consolidation of bands after phosphatase treatment indicates that phosphorylation is a major post-translational modification for both 3R and 4R tau isoforms.

In brain homogenates of 12-15 week-old naïve rats (Figure 2B), the staining for both 4R and 3R tau isoforms largely is similar to that of the six week-old naïve rats. The main difference is the qualitative decrease in 0N3R expression in brain homogenates from 12-15 week-old rats compared to the younger rats. When comparing 0N3R tau from 12-15 weeks old naïve rats to bands in the *human tau ladder lane* (where each band is 10 ng), the 0N3R band is much lighter in intensity. This observation contrasts with 3R staining from six week-old rats (Figure 2A), where the intensity of 0N3R is similar in brightness to bands in the *human tau ladder*. This progressive reduction in 0N3R band intensity suggests a developmental down regulation of this specific tau isoform, consistent with a previous report (Hanes et al, 2009).

We next looked at expression of phosphorylated S193/T196 (pS193/pT196) tau by using the AT8 Ab in brain homogenates of 12-15 week-old naïve rats (Figure 2C). In human AD, S202/T205 hyperphosphorylation is widely used as a biomarker of AD (Braak & Braak, 1991). We validated this Ab's phosphospecific recognition of tau by observing the 75 kDa staining of the phosphorylated 2N4R human tau species as a positive control (*h. p2N4R tau*) and the absence of staining in the nonphosphorylated *human tau ladder* lane, as a negative control. We observed three distinct bands of pS193/pT196 tau, ranging from approximately 58-72 kDa (*boxes* in Figure 2C). Compared to the migration of dephosphorylated rat tau isoforms shown in Figures 2A & 2B, these bands likely consist of 2N4R and 1N4R tau with varying degrees of phosphorylation. Both 0N3R and 0N4R tau isoforms migrate around 50 kDa, but these tau isoforms were not observed when probing for pS193/pT196 tau species. Taken together, AT8 staining is mainly composed of 1N4R and 2N4R tau isoforms.

In addition to pS193/pT196 tau staining, we detected total tau expression levels in brain lysates from 12-15 week-old naïve rats by western blotting using the Tau-5 Ab (Figure 2D). This Ab recognizes all six tau isoforms in the human tau ladder (*h. tau ladder*), which served as a positive control. When examining brain homogenates from 12-15 week-old naïve rats, total tau staining ranged from 50-72 kDa and appeared as four distinct bands, as shown in Figure 2D. Upon phosphatase treatment, we observed three distinct bands. Comparing the total tau staining between the two conditions, it appears that: the bottom band in the *(+)pptase lane* is composed of 0N tau and corresponds to the bottom box within raw homogenates; the middle band in the *(+)pptase lane* is composed of 1N4R tau and correlates to the second and third boxes from the bottom within raw lysates, demonstrating differing levels of phosphorylation of the 1NR isoform; and the upper band in the *(+)pptase lane* is composed of 2N4R tau and migrates within the third and fourth boxes from the bottom in raw lysates, indicating differing 2N4R phosphorylation levels. Consistent with the observed reduction in 0N3R tau expression in 12-15 week-old rats together with the minimal expression levels of both 1N3R and 2N3R, total tau staining reflects only 4R tau expression. This observation is supported by complete overlapping of total tau expression staining with 4R tau staining (Figure 2E).

Tau expression in chronic epilepsy

After establishing the expression pattern of tau isoforms by western blotting, we investigated changes in expression in the hippocampus of chronically epileptic rats of total tau, pS193/pT196 tau, and two other phosphorylated tau species that are hyperphosphorylated in AD, pT172 tau (rat ortholog of human pT181 tau) and pT222 tau (rat ortholog of human pT231 tau). The use of western blotting with age-matched naïve and epileptic conditions assessed within the same blot allowed for quantification of changes in these various tau species in epilepsy. Quantification of the change in tau expression between epileptic and naive conditions within the same blot normalizes for differences in antibody binding, imaging efficiency, etc. that occur between experiments; thus what is quantified is the percent change in tau expression between epileptic and naïve conditions. As described in Methods, three doubling amounts of proteins were loaded from each sample to ensure signal detection occurred within a linear range (Jung et al., 2010; Tai et al., 2017; Parikh et al., 2020; Concepcion et al., 2021). Also included were appropriate (+) and (−) controls in each gel to validate Ab specificity. Lastly, we measured aggregate expression of all tau isoforms ranging between 50-72 kDa, rather than individual bands.

We studied two time points during chronic epilepsy, two months and four months post-SE. We have shown in prior work (Tai et al., 2017) that at two months post-SE, rats have frequent seizures (4.0 ± 1.1 seizures/day, $n = 11$), ranging from focal motor manifestations (Racine class III) to convulsions with loss of posture (class V). To verify that our chronically epileptic rats were experiencing seizures at the four month post-SE time point, we video-monitored four chronically epileptic rats for two continuous weeks. These rats averaged 10.9 ± 3.65 Racine class III-V seizures/day ($p = 0.03$ vs. two months post-SE). This monitoring not only established that four month post-SE rats experience class III-V seizures but also demonstrated a progressive increase in seizure frequency compared to two month post-SE rats. Because seizures in the pilocarpine model of temporal lobe epilepsy (TLE)

predominantly originate within the hippocampus (Toyoda et al., 2013; Buckmaster et al., 2022), we looked at the whole hippocampal formation (including the subiculum and entorhinal cortex) as well as two subregions separately, CA1 and CA3 hippocampus. A brain region outside the putative seizure onset site, the somatosensory cortex (SSC), served as a control region (Figure 1C).

In two months post-SE chronically epileptic rats (Figure 4), individual hippocampal subfields showed decreased levels of pS193/pT196 tau (CA1: 30.3 ± 9.51% reduction compared to controls, $n = 10$, $p = 0.011$; CA3: 35.5 ± 12.6% reduction, $n = 11$, $p = 0.018$), but no significant change in pS193/pT196 tau was seen in the hippocampal formation as a whole (18.1 ± 11.0% reduction, $n = 10$, $p > 0.05$) or in the nonepileptogenic SSC (9.5 ± 14.8% increase compared to controls, $n = 9$, $p > 0.05$). With total tau expression levels, we observed a decline compared to controls in every region, including the SSC (whole hippocampus: 20.6 ± 3.06% reduction, $n = 10$, $p < 0.0001$; CA1: 24.7 ± 4.88% reduction, $n = 10$, $p = 0.0007$; CA3: 25.1 ± 7.00% reduction, $n = 11$, $p = 0.005$; SSC: 15.7 ± 4.56% reduction, $n = 9$, $p = 0.0088$). These results demonstrated that in the early stages of chronic epilepsy, a modest uniform loss of total tau expression took place throughout the whole hippocampus (and SSC), while losses of pS193/pT196 tau levels occurred in the CA1 and CA3 hippocampal subfields, but not in the hippocampus as a whole or in the SSC. Because the decrease in phosphorylated tau species in the CA1 and CA3 subregions largely was comparable to the decrease in total tau expression, the fractional phosphorylation of pS193/pT196 tau was unchanged in the CA1 subfield (8.35 ± 10.3% reduction compared to controls, $n = 10$, $p > 0.05$) and the CA3 subfield (14.5 ± 11.6% reduction compared to controls, $n = 11$, $p > 0.05$). Thus, the observed reductions in pS193/pT196 tau can be explained by decreases in total tau expression occurring throughout the hippocampus.

At four months post-SE (Figure 5), when the chronically epileptic rats were experiencing a significantly higher rate of spontaneous seizures as compared to two month post-SE animals, there was a significant decrease in pS193/pT196 tau in the whole hippocampal formation (45.0 ± 7.53% reduction compared to age-matched controls, $n = 11$, $p < 0.0001$), in contrast with the earlier time point. Significant losses in pS193/pT196 tau also were observed in both hippocampal subregions: CA1: 24.8 ± 6.39% reduction, $n = 10$, $p = 0.0037$; CA3: 49.8 ± 5.88% reduction, $n = 10$, $p < 0.0001$. No change in pS193/pT196 tau was observed in the SSC, like the earlier time point. When examining total tau expression there was a modest decrease in the CA3 hippocampus (22.8 ± 5.82% reduction, $n = 10$, $p = 0.0035$), but the losses in total tau protein seen earlier in the whole hippocampal formation, CA1, and SSC were not observed in the four month post-SE rats.

Fractional phosphorylation of pS193/pT196 tau revealed significant reductions in the whole hippocampal formation (39.4 ± 10.5% reduction compared to controls, $n = 11$, $p = 0.0038$) and in the CA3 hippocampus (32.4 ± 7.90% reduction, $n = 10$, $p = 0.0027$), but not in the CA1 hippocampus (6.72 ± 8.99% reduction, $n = 10$, $p > 0.05$) and SSC control region (6.68 ± 8.51% reduction, $n = 10$, $p > 0.05$). These reductions in fractional phosphorylation levels in both whole hippocampus and CA3 hippocampus imply changes in upstream phosphorylation signaling and are not due to loss of total tau expression alone.

We also studied two other canonical phosphosites on tau that are used as molecular biomarkers in AD: T181 (T172 in rat) and T231 (T222 in rat). Both of these phosphosites are known to be hyperphosphorylated in AD (Suárez-Calvet et al., 2020). In the whole hippocampal formation at four months post-SE, we looked at both pT172 tau expression with the AT270 Ab and pT222 tau expression with the 1H6L6 Ab (Figure 5C). For both phosphorylated tau species, we found no changes in either phosphorylation levels (pT172: 15.4 ± 15.9% reduction, $n = 11$, $p > 0.05$; pT222: 8.84 ± 13.9% reduction, $n = 11$, $p > 0.05$) or fractional phosphorylation (pT172: 15.1 ± 11.4% reduction, $n = 11$, $p > 0.05$; pT222: 1.26 ± 16.9% reduction, $n = 11$, $p > 0.05$). Therefore, addressing the three canonical tau phosphosite loci that are hyperphosphorylated in AD, there was no evidence of hyperphosphorylation at the two stages of chronic epilepsy in our rat model of TLE. Rather, the S193/T196 tau locus showed dephosphorylation that progressed during chronic epilepsy and was due to a fractional loss of tau phosphorylation.

Localization of dual pS193/pT196 tau

Because the greatest changes in pS193/pT196 tau were observed at the four month post-SE stage, we asked where pS193/pT196 tau is expressed within the hippocampus and whether there are changes in the subcellular distribution of this phosphorylated tau species in these chronically epileptic rats. We investigated pS193/pT196 tau localization within the CA1 hippocampus (Figure 6) and CA3 hippocampus (Figure 7) by performing immunohistochemistry (IHC) with the AT8 Ab in four month post-SE rats and age-matched naïve rats. Within the CA1 hippocampus of naïve rats we observed the brightest staining within the *stratum (s.) pyramidale* layer that corresponds to the somata of hippocampal pyramidal neurons; modest staining within the dendrites that begins at the *s. radiatum* layer; and minimal staining in the axonal *s. oriens* layer (Figure 6A-D). Additionally, we observed a consistent qualitative increased dendritic brightness when transitioning to the CA3 hippocampus from the CA1 hippocampus (* in Figure 6A).

A similar pS193/pT196 tau staining pattern was seen within the CA1 hippocampus of chronically epileptic rats (Figure 6E-H), in which staining was greatest in the somata, lower in the dendritic subcellular layer, and little to no detection in the *s. oriens* layer. To investigate changes in the subcellular distribution of pS193/pT196 tau, we compared the ratio of signal intensity per unit area between the somatic and dendritic layers from CA1 subcellular regions between four month-post-SE rats and their age-matched controls. No difference in the ratio of somatic/dendritic staining was detected: [1.24 ± 0.05 in chronics ($n = 4$), 1.33 ± 0.02 in controls ($n = 3$); $p > 0.05$]. However, overall staining for pS193/pT196 tau qualitatively was lower in the chronically epileptic rats than in the control rats.

Addressing pS193/pT196 tau localization within the CA3 hippocampus, we noticed in the age-matched control rats (Figure 7A-D): the strongest staining of pS193/pT196 tau occurs in the *s. lucidum* layer that corresponds to the mossy fiber projections from the dentate gyrus and in the somata of hippocampal pyramidal neurons (*s. pyramidale*); somewhat less staining in the dendritic (*s. radiatum)* layer; and the least expression in the axons of the *s. oriens* layer (Figure 7A-D). Similar to the previous observation at the transition between the CA1 hippocampus and the CA3 hippocampus, there appears to be a reduction in the dually

phosphorylated tau staining in the dendritic layer of the CA1 subregion compared to that of the CA3 subregion. Therefore, both observations in Figure 6A and Figure 7A suggest that under normal conditions pS193/pT196 tau staining appears to become higher in the CA3 hippocampus dendritic layer than that of the CA1 hippocampus at this transition zone.

In four month post-SE rats (Figure 7E-H), although there appears to be a general reduction in overall pS193/pT196 tau staining compared to the age-matched naives, the overall dually phosphorylated tau pattern was similar to the controls in terms of relative comparisons of staining intensities among different subcellular compartments (mossy fiber and somata > dendrites > *s. oriens*). Like the CA1 hippocampus analysis, we investigated changes in staining ratios between various subcellular compartments: (A) somatic vs. dendritic; (B) somatic vs. s. lucidum; and (C) s. lucidum vs. dendritic. For all three comparisons, no differences were observed: [somatic/dendritic: 1.23 ± 0.04 in chronics, (n = 4), 1.06 ± 0.05 in naives, (n = 3), p > 0.05; somatic/s. lucidum: 0.99 ± 0.07 in chronics, (n = 4), 0.88 ± 0.01 in naives, (n = 3), p > 0.05; and s. lucidum/dendritic: 1.27 ± 0.10 in chronics, (n = 4), 1.21 ± 0.07 in naives, (n = 3), p > 0.05]. Despite the absence of changes in staining ratios, there is an apparent overall reduction in pS193/pT196 tau within the CA3 hippocampus of chronically epileptic rats compared to age-matched naives. Interestingly, these qualitative decreases in pS193/pT196 tau in this stage of chronic epilepsy reflect the quantitative reductions in this dually phosphorylated tau species seen in the western blotting experiments (Figure 4).

Discussion

There is increasing interest in understanding whether the neurodegeneration often occurring in the temporal lobe of patients with TLE is mediated by similar mechanisms as in AD, such as tau hyperphosphorylation, increases in beta-amyloid deposition, or neuroinflammation (Casillas-Espinosa et al., 2020; Hwang et al., 2022). Observations in human brain tissue from patients with refractory epilepsy have been conflicting as to whether tau expression and phosphorylation are increased as they are in patients with AD; while studies in animal models show that tau expression is necessary for the occurrence of seizures in genetic models of epilepsy, and that deletion or knockdown of tau exerts an anti-seizure effect. Our goal here was to examine tau expression and phosphorylation at three canonical phosphosites that are hyperphosphorylated in AD (and consequently used in the clinical diagnosis of AD) by using a well-validated animal model of temporal lobe epilepsy. We evaluated these tau properties in the brain regions where seizures arise, and also a region outside of the epileptogenic zone, at two time points of chronic epilepsy equivalent to years of exposure to seizures in humans. A strength of our approach is studying these epileptic animals at two points, especially a late time point at four months post-induction of epilepsy with a high cumulative seizure burden comparable to that in humans with many years of refractory epilepsy (Wiebe et al., 2001). Our most important finding is that tau is progressively dephosphorylated at the rat S193/T196 loci (equivalent to the S202/T205 tau loci in humans assayed by the AT8 antibody) as the epileptic state progresses, with no change in overall tau expression at the latter timepoint of chronic epilepsy. Two other tau phosphosites implicated in AD, orthologs of human T181 and T231, showed no change in phosphorylation. These results demonstrate that three canonical phosphosites

showing hyperphosphorylation in AD do not show hyperphosphorylation in late stages of chronic epilepsy in an animal model of TLE, and that the dephosphorylation at S193/T196 progressively increased as epilepsy worsened over time.

At two months post-SE, our prior work established that rats are experiencing about four Racine class III-V (focal motor or convulsive) seizures per day (Tai et al., 2017). Given that humans with refractory temporal lobe epilepsy experience about three seizures per month (Wiebe et al., 2001), if this were the steady-state rate of seizures in rats, it would be equivalent to several years' duration of epilepsy in humans. At this time point, we found proportional losses of both total tau expression and pS193/pT196 tau levels in the hippocampus. The proportional loss of phosphorylated tau implied that it reflects the loss of total tau expression, with no changes in fractional phosphorylation in all investigated hippocampal fields. Interestingly, we observed decreased total tau expression in every hippocampal region studied, as well as the SSC region outside of the putative onset seizure site, suggesting an ongoing compensatory mechanism not only in the affected hippocampal formation but also surrounding brain regions, given that loss of total tau expression has an antiepileptic effect (Holth et al., 2013; Gheyara et al., 2014). Since the changes in total tau expression seen in our model largely reverted to normal at the four month post-SE time point, including outside of the epileptogenic zone in the SSC, they are unlikely to be due to neurodegeneration but rather to a homeostatic process throughout the brain in response to ongoing seizures.

At the later time point four months post-SE, we observed a much higher convulsive seizure rate of 10 per day, equivalent at steady state to many years of seizure exposure in humans, such as occurs in patients who present for epilepsy surgical interventions after numerous years of uncontrolled seizures (Wiebe et al., 2001). At this time point as mentioned above, total tau expression in the hippocampus as a whole had normalized compared to its modest decline at two months post-SE. This shows that there is no progressive upregulation of total tau expression with long exposure to epilepsy in our model. In contrast, there was a progressive loss of phosphorylation at the S193/T196 tau loci – an ~50% loss of phosphorylation was seen in the hippocampal formation as a whole and in the CA3 region specifically, with a lesser degree seen in the CA1 region. Because this loss of S193/T196 tau phosphorylation occurred in the setting of unchanged total tau expression in the hippocampus as a whole, it represented a loss of fractional phosphorylation of tau from upstream phosphorylation signaling and would not be explained by loss of neurons in the hippocampus. A control region outside of the hippocampus, the SSC, showed no change in tau phosphorylation, demonstrating that this change was specific to the epileptogenic zone. Immunohistochemistry studies at the four mo. post-SE time point showed that tau phosphorylated at S193/T196 was mostly expressed in hippocampal pyramidal neuron somas and dendrites and mossy fibers, and showed a qualitative decrease in expression vs. age-matched controls, mirroring the quantitative changes found with the western blotting analyses. It has shown that anesthesia may influence the phosphorylation of tau at various phosphosites, including T181 and T205 (Run et al., 2009). However, changes in tau phosphorylation described here were not due to anesthesia, given that both cohorts received the same anesthesia treatment (although it is possible that anesthesia could influence the subcellular distribution seen under both conditions).

The decreased tau phosphorylation at S193/T196 tau in our rat model differed from a prior study using a kainic acid (KA) model of epilepsy evaluated at 14 days post-SE (Alves et al., 2019). This study found increased tau phosphorylation at this locus and decreased total tau expression. However, this time point represents a much earlier phase of epilepsy, so it is possible that this result is not comparable to later, more chronic phases of epilepsy investigated here. Their study did detect total tau reductions in the CA1 and CA3 hippocampal subfields as we did in our earlier time point at two months post-induction of epilepsy. Another study used two different modes of KA delivery to induce epileptogenesis, intrahippocampal vs. intraperitoneal injections (Canet et al., 2022). With intrahippocampal KA delivery, several tau phosphosites (orthologous to human tau T212/ S214, S396/S404, and S202 loci) were hyperphosphorylated at eight weeks post-injection. With intraperitoneal KA delivery, only the T212/ S214 loci showed hyperphosphorylation at eight weeks post-SE time point. In this study, total tau expression was not quantified (so it is unclear whether these changes in phosphorylation represented fractionally increased phosphorylation or increased total tau expression), but the findings do demonstrate some model-dependence of the changes seen. Their study also noted varying time dependent trajectories of expression of neuroinflammatory and neurogenerative mediators aside from changes in tau phosphorylation. Our study examined the phosphorylation levels of three tau phosphorylation loci, accounting for just four of 85 possible phosphosites in the 2N4R human tau isoform expressed in the brain (Wang & Mandelkow, 2016). The phosphorylation changes were non-uniform among these three loci, and thus it is certainly possible that other tau phosphosites not assayed here may undergo increased phosphorylation as was seen in the prior study.

In terms of comparison to human post-mortem or resection studies assaying tau expression and phosphorylation in patients with refractory epilepsy, corroboration of our finding occurred in a study involving IHC measurements of tau in autopsy specimens from patients with refractory epilepsy: the sclerotic hippocampus at the putative site of seizure onset showed a loss of pS202/pT205 tau staining compared to the non-sclerotic contralateral hippocampus (Thom et al., 2011). Other human studies have reached conflicting conclusions, finding either increased total and phosphorylated tau expression in resection (Tai et al., 2016) or post-mortem tissue (Gourmaud et al., 2020) or no change in S202/T205 tau phosphorylation in resection tissue (Silva et al., 2021). A significant challenge in human tissue studies is comparison to a suitable control sample: usually this is an autopsy specimen from a human brain bank, but conditions for handling this tissue may differ from those for the epilepsy specimens, and it is known that tau protein phosphorylation decays within hours of brain death in both humans and rats (Matsuo et al., 1994; Gärtner et al., 1998). Thus, brain banked control tissue may have artifactually low levels of tau phosphorylation. A methodology which partially circumvents this technical issue is measurement of tau expression in CSF. One study using this technique in a small group of patients of heterogeneous seizure etiologies found no significant change in total tau expression or phosphorylation at the S181 phosphosite when studied 48 hours after a recent seizure (Palmio et al., 2009).

Like humans, rats express six tau isoforms in the brain. However, we found that isoform expression in rats is non-uniform. We readily detected only four tau isoforms (0N3R, 0N4R,

1N4R, and 2N4R); additionally, we showed that most of the tau protein in rat hippocampus was 4R tau species, consistent with the 7:1 ratio of 4R:3R tau expression reported in three month-old rat hippocampus (Hanes et al., 2009). We also showed that not all tau isoforms are phosphorylated equally. As seen by western blotting patterns in Figure 2C, pS193/pT196 tau appeared to originate from 1N4R and 2N4R tau isoforms, but not 0N4R tau. These results suggested that expression changes of total and phosphorylated tau in epilepsy may be confined to a subset of the six possible tau isoforms.

It is unclear how loss of tau phosphorylation at the S193/T196 phosphosites impacts its biological role in brain tissue. It has been tacitly assumed that hyperphosphorylation of tau in epilepsy causes loss of biological function and neurotoxicity as is seen in AD. However, this may not necessarily be so. Changes in phosphorylation at individual phosphosites may have differing impacts on tau function as relates to neuronal excitability and seizure generation. A recent study showed that while genetic deletion of tau reduced the intrinsic excitability of hippocampal neurons, expression of phosphorylated human tau in the absence of endogenous murine tau also produced hypoexcitability (Cloyd et al., 2021). This suggests that the effects of tau phosphorylation on neuronal excitability may be complex and not follow the AD model. In AD, hyperphosphorylation of tau appears to occur in a sequential fashion, implying complex interactions among upstream signaling pathways (Luna-Muñoz et al., 2007; Bertrand et al., 2010). As we learn more about the many tau phosphosites that could be dysregulated in refractory epilepsy, this could be an interesting area of investigation.

What is the cause of tau dephosphorylation at S193/T196 in late chronic epilepsy? It is possible that it is the result of the epileptogenic processes underlying seizure generation in the hippocampus. Alternatively, tau dephosphorylation could be a consequence of neurodegeneration in the hippocampus that accompanies refractory epilepsy (Casillas-Espinosa et al., 2020), even if dissimilar to the hyperphosphorylation of tau accompanying neurodegeneration in AD. Experiments to determine the seizure dependence of tau phosphorylation in animals with chronic epilepsy (using treatment with anti-seizure medications in vivo) could be informative. Of note, the loss of fractional phosphorylation at S193/T196 at four months post-SE does not reflect loss of neurons per se, since total tau expression was unchanged. Another interesting question is whether tau expression is altered in the early stages of epileptogenesis post-SE but before spontaneous seizures arise (about one week post-SE in our model), a question that was outside the scope of this investigation.

We feel these results warrant further comprehensive examination of phosphorylation at other tau phosphosites in chronic epilepsy. Use of acquired epilepsy models such as the pilocarpine-induced rat model used here at late time points of chronic epilepsy may accurately model the human condition in chronic medically refractory epilepsy, but it would be worthwhile to study tau expression in other animal models. Such experiments will help determine whether tau undergoes net hyperphosphorylation or dephosphorylation in epilepsy, or whether changes in phosphorylation at individual phosphosites have unique contributions to neuronal excitability and neurodegeneration.

Acknowledgments

This work was supported by the National Institute of Neurological Disorders and Stroke (NS050229) and by a Seed Grant from the American Epilepsy Society. We thank Tessandra Stewart, PhD, Department of Laboratory Medicine and Pathology, University of Washington, for her invaluable guidance and contributions to this research paper.

References

Alves M, Kenny A, de Leo G, Beamer EH, & Engel T (2019). Tau Phosphorylation in a Mouse Model of Temporal Lobe Epilepsy. Front Aging Neurosci, 11, 308. doi:10.3389/fnagi.2019.00308 [PubMed: 31780921]

Aroor A, Nguyen P, Li Y, Das R, Lugo JN, and Brewster AL. Assessment of tau phosphorylation and β-amyloid pathology in human drug-resistant epilepsy. Epilepsia Open, in press.

Bertrand J, Plouffe V, Sénéchal P, & Leclerc N (2010). The pattern of human tau phosphorylation is the result of priming and feedback events in primary hippocampal neurons. Neuroscience, 168(2), 323–334. doi:10.1016/j.neuroscience.2010.04.009 [PubMed: 20394726]

Braak H, & Braak E (1991). Neuropathological stageing of Alzheimer-related changes. Acta Neuropathol, 82(4), 239–259. doi:10.1007/BF00308809 [PubMed: 1759558]

Buckmaster PS, Reyes B, Kahn T, & Wyeth M (2022). Ventral hippocampal formation is the primary epileptogenic zone in a rat model of temporal lobe epilepsy. J Neurosci, 42(39), 7482–7495. doi:10.1523/JNEUROSCI.0429-22.2022 [PubMed: 35995562]

Canet G, Zub E, Zussy C, Hernandez C, Blaquiere M, Garcia V, Vitalis M, deBock F, Moreno-Montano M, Audinat E, Desrumaux C, Planel E, Givalois L, & Marchi N (2022). Seizure activity triggers tau hyperphosphorylation and amyloidogenic pathways. Epilepsia, 63(4), 919–935. doi:10.1111/epi.17186 [PubMed: 35224720]

Casillas-Espinosa PM, Ali I, & O'Brien TJ (2020). Neurodegenerative pathways as targets for acquired epilepsy therapy development. Epilepsia Open, 5(2), 138–154. doi:10.1002/epi4.12386 [PubMed: 32524040]

Chen C, Holth JK, Bunton-Stasyshyn R, Anumonwo CK, Meisler MH, Noebels JL, & Isom LL (2018). Mapt deletion fails to rescue premature lethality in two models of sodium channel epilepsy. Ann Clin Transl Neurol, 5(8), 982–987. doi:10.1002/acn3.599 [PubMed: 30128323]

Cloyd RA, Koren J, Abisambra JF, & Smith BN (2021). Effects of altered tau expression on dentate granule cell excitability in mice. Exp Neurol, 343, 113766. doi:10.1016/j.expneurol.2021.113766 [PubMed: 34029610]

Concepcion FA, Khan MN, Ju Wang JD, Wei AD, Ojemann JG, Ko AL, Shi Y, Eng JK, Ramirez JM, & Poolos NP (2021). HCN Channel Phosphorylation Sites Mapped by Mass Spectrometry in Human Epilepsy Patients and in an Animal Model of Temporal Lobe Epilepsy. Neuroscience, 460, 13–30. doi:10.1016/j.neuroscience.2021.01.038 [PubMed: 33571596]

Curia G, Longo D, Biagini G, Jones RS, & Avoli M (2008). The pilocarpine model of temporal lobe epilepsy. J Neurosci Methods, 172(2), 143–157. doi:10.1016/j.jneumeth.2008.04.019 [PubMed: 18550176]

DeVos SL, Goncharoff DK, Chen G, Kebodeaux CS, Yamada K, Stewart FR, Schuler DR, Maloney SE, Wozniak DF, Rigo F, Bennett CF, Cirrito JR, Holtzman DM, & Miller TM (2013). Antisense reduction of tau in adult mice protects against seizures. J Neurosci, 33(31), 12887–12897. doi:10.1523/JNEUROSCI.2107-13.2013 [PubMed: 23904623]

Gärtner U, Janke C, Holzer M, Vanmechelen E, & Arendt T (1998). Postmortem changes in the phosphorylation state of tau-protein in the rat brain. Neurobiol Aging, 19(6), 535–543. doi:10.1016/s0197-4580(98)00094-3 [PubMed: 10192212]

Gheyara AL, Ponnusamy R, Djukic B, Craft RJ, Ho K, Guo W, Finucane MM, Sanchez PE, & Mucke L (2014). Tau reduction prevents disease in a mouse model of Dravet syndrome. Ann Neurol, 76(3), 443–456. doi:10.1002/ana.24230 [PubMed: 25042160]

Gourmaud S, Shou H, Irwin DJ, Sansalone K, Jacobs LM, Lucas TH, Marsh ED, Davis KA, Jensen FE, & Talos DM (2020). Alzheimer-like amyloid and tau alterations associated with cognitive deficit in temporal lobe epilepsy. Brain, 143(1), 191–209. doi:10.1093/brain/awz381 [PubMed: 31834353]

Hanes J, Zilka N, Bartkova M, Caletkova M, Dobrota D, & Novak M (2009). Rat tau proteome consists of six tau isoforms: implication for animal models of human tauopathies. J Neurochem, 108(5), 1167–1176. doi:10.1111/j.1471-4159.2009.05869.x [PubMed: 19141083]

Hatch RJ, Wei Y, Xia D, & Götz J (2017). Hyperphosphorylated tau causes reduced hippocampal CA1 excitability by relocating the axon initial segment. Acta Neuropathol, 133(5), 717–730. doi:10.1007/s00401-017-1674-1 [PubMed: 28091722]

Holth JK, Bomben VC, Reed JG, Inoue T, Younkin L, Younkin SG, Pautler RG, Botas J, & Noebels JL (2013). Tau loss attenuates neuronal network hyperexcitability in mouse and Drosophila genetic models of epilepsy. J Neurosci, 33(4), 1651–1659. doi:10.1523/JNEUROSCI.3191-12.2013 [PubMed: 23345237]

Hwang K, Vaknalli RN, Addo-Osafo K, Vicente M, & Vossel K (2022). Tauopathy and Epilepsy Comorbidities and Underlying Mechanisms. Front Aging Neurosci, 14, 903973. doi:10.3389/fnagi.2022.903973 [PubMed: 35923547]

Jung S, Jones TD, Lugo JN, Sheerin AH, Miller JW, D'Ambrosio R, Anderson AE, & Poolos NP (2007). Progressive dendritic HCN channelopathy during epileptogenesis in the rat pilocarpine model of epilepsy. J Neurosci, 27(47), 13012–13021. doi:10.1523/JNEUROSCI.3605-07.2007 [PubMed: 18032674]

Jung S, Bullis JB, Lau IH, Jones TD, Warner LN, & Poolos NP (2010). Downregulation of dendritic HCN channel gating in epilepsy is mediated by altered phosphorylation signalling. J Neurosci, 30, 6678–6688. [PubMed: 20463230]

Li C, & Götz J (2017). Tau-based therapies in neurodegeneration: opportunities and challenges. Nat Rev Drug Discov, 16(12), 863–883. doi:10.1038/nrd.2017.155 [PubMed: 28983098]

Luna-Muñoz J, Chávez-Macías L, García-Sierra F, & Mena R (2007). Earliest stages of tau conformational changes are related to the appearance of a sequence of specific phospho-dependent tau epitopes in Alzheimer's disease. J Alzheimers Dis, 12(4), 365–375. doi:10.3233/jad-2007-12410 [PubMed: 18198423]

Matsuo ES, Shin RW, Billingsley ML, Van deVoorde A, O'Connor M, Trojanowski JQ, & Lee VM (1994). Biopsy-derived adult human brain tau is phosphorylated at many of the same sites as Alzheimer's disease paired helical filament tau. Neuron, 13(4), 989–1002. doi:10.1016/0896-6273(94)90264-x [PubMed: 7946342]

Medeiros R, Baglietto-Vargas D, & LaFerla FM (2011). The role of tau in Alzheimer's disease and related disorders. CNS Neurosci Ther, 17(5), 514–524. doi:10.1111/j.1755-5949.2010.00177.x [PubMed: 20553310]

Mo L, Ding X, Tan C, Liu X, Wei X, Wang H, Zhou W, & Chen L (2019). Association of cerebrospinal fluid zinc-α2-glycoprotein and tau protein with temporal lobe epilepsy and related white matter impairment. Neuroreport, 30(8), 586–591. doi:10.1097/WNR.0000000000001252 [PubMed: 30964766]

Palmio J, Suhonen J, Keränen T, Hulkkonen J, Peltola J, & Pirttilä T (2009). Cerebrospinal fluid tau as a marker of neuronal damage after epileptic seizure. Seizure, 18(7), 474–477. doi:10.1016/j.seizure.2009.04.006 [PubMed: 19428269]

Parikh AN, Concepcion FA, Khan MN, Boehm RD, Poolos OC, Dhami A, & Poolos NP (2020). Selective hyperactivation of JNK2 in an animal model of temporal lobe epilepsy. IBRO Rep, 8, 48–55. doi:10.1016/j.ibror.2020.01.001 [PubMed: 32072069]

Roberson ED, English JD, Adams JP, Selcher JC, Kondratick C, & Sweatt JD (1999). The mitogen-activated protein kinase cascade couples PKA and PKC to cAMP response element binding protein phosphorylation in area CA1 of hippocampus. J Neurosci, 19(11), 4337–4348. [PubMed: 10341237]

Romoli M, Sen A, Parnetti L, Calabresi P, & Costa C (2021). Amyloid-β: a potential link between epilepsy and cognitive decline. Nat Rev Neurol, 17(8), 469–485. [PubMed: 34117482]

Run X, Liang Z, Zhang L, Iqbal K, Grundke-Iqbal I, & Gong CX (2009). Anesthesia induces phosphorylation of tau. J Alzheimers Dis, 16(3), 619–626. doi:10.3233/JAD-2009-1003 [PubMed: 19276556]

Sen A, Thom M, Martinian L, Harding B, Cross JH, Nikolic M, & Sisodiya SM (2007). Pathological tau tangles localize to focal cortical dysplasia in older patients. Epilepsia, 48(8), 1447–1454. doi:10.1111/j.1528-1167.2007.01107.x [PubMed: 17441989]

Shao E, Chang CW, Li Z, Yu X, Ho K, Zhang M, Wang X, Simms J, Lo I, Speckart J, Holtzman J, Yu GQ, Roberson ED, & Mucke L (2022). TAU ablation in excitatory neurons and postnatal TAU knockdown reduce epilepsy, SUDEP, and autism behaviors in a Dravet syndrome model. Sci Transl Med, 14(642), eabm5527. doi:10.1126/scitranslmed.abm5527 [PubMed: 35476595]

Silva JC, Vivash L, Malpas CB, Hao Y, McLean C, Chen Z, O'Brien TJ, Jones NC, & Kwan P (2021). Low prevalence of amyloid and tau pathology in drug-resistant temporal lobe epilepsy. Epilepsia, 62(12), 3058–3067. doi:10.1111/epi.17086 [PubMed: 34595752]

Smith KM, Blessing MM, Parisi JE, Britton JW, Mandrekar J, & Cascino GD (2019). Tau deposition in young adults with drug-resistant focal epilepsy. Epilepsia, 60(12), 2398–2403. doi:10.1111/epi.16375 [PubMed: 31663115]

Suárez-Calvet M, Karikari TK, Ashton NJ, Lantero Rodríguez J, Milà-Alomà M, Gispert JD, Salvadó G, Minguillon C, Fauria K, Shekari M, Grau-Rivera O, Arenaza-Urquijo EM, Sala-Vila A, Sánchez-Benavides G, González-de-Echávarri JM, Kollmorgen G, Stoops E, Vanmechelen E, Zetterberg H, Blennow K, Molinuevo JL, & ALFA S (2020). Novel tau biomarkers phosphorylated at T181, T217 or T231 rise in the initial stages of the preclinical Alzheimer's continuum when only subtle changes in Aβ pathology are detected. EMBO Mol Med, 12(12), e12921. doi:10.15252/emmm.202012921 [PubMed: 33169916]

Tai TY, Warner LN, Jones TD, Jung S, Skyrud DW, Fender J, Liu Y, Williams AD, Neumaier JF, D'Ambrosio R, & Poolos NP (2017). Antiepileptic action of c-Jun-N-terminal kinase (JNK) inhibition in an animal model of epilepsy. Neuroscience, 349, 35–47. [PubMed: 28237815]

Tai XY, Koepp M, Duncan JS, Fox N, Thompson P, Baxendale S, Liu JY, Reeves C, Michalak Z, & Thom M (2016). Hyperphosphorylated tau in patients with refractory epilepsy correlates with cognitive decline: a study of temporal lobe resections. Brain, 139(Pt 9), 2441–2455. doi:10.1093/brain/aww187 [PubMed: 27497924]

Thom M, Liu JY, Thompson P, Phadke R, Narkiewicz M, Martinian L, Marsdon D, Koepp M, Caboclo L, Catarino CB, & Sisodiya SM (2011). Neurofibrillary tangle pathology and Braak staging in chronic epilepsy in relation to traumatic brain injury and hippocampal sclerosis: a post-mortem study. Brain, 134(Pt 10), 2969–2981. doi:10.1093/brain/awr209 [PubMed: 21903728]

Toyoda I, Bower MR, Leyva F, & Buckmaster PS (2013). Early activation of ventral hippocampus and subiculum during spontaneous seizures in a rat model of temporal lobe epilepsy. J Neurosci, 33(27), 11100–11115. doi:10.1523/JNEUROSCI.0472-13.2013 [PubMed: 23825415]

Wang JZ, Xia YY, Grundke-Iqbal I, & Iqbal K (2013). Abnormal hyperphosphorylation of tau: sites, regulation, and molecular mechanism of neurofibrillary degeneration. J Alzheimers Dis, 33 Suppl 1, S123–39. doi:10.3233/JAD-2012-129031 [PubMed: 22710920]

Wang Y, & Mandelkow E (2016). Tau in physiology and pathology. Nat Rev Neurosci, 17(1), 5–21. doi:10.1038/nrn.2015.1 [PubMed: 26631930]

Wiebe S, Blume WT, Girvin JP, & Eliasziw M (2001). A randomized, controlled trial of surgery for temporal-lobe epilepsy. N Engl J Med, 345(5), 311–318. doi:10.1056/NEJM200108023450501 [PubMed: 11484687]

Williams AD, Jung S, & Poolos NP (2015). Protein kinase C bidirectionally modulates Ih and hyperpolarization-activated cyclic nucleotide-gated (HCN) channel surface expression in hippocampal pyramidal neurons. J Physiol, 593(13), 2779–2792. doi:10.1113/JP270453 [PubMed: 25820761]

Highlights

- S193/T196 (S202/T205 human) tau showed progressive dephosphorylation in epilepsy.
- No change in phosphorylation at T172 (T181 human) or T222 (T231 human) was seen.
- At 2 months post-SE, total tau expression was transiently decreased.
- Tau expression and phosphorylation at 3 loci differ between chronic epilepsy and AD

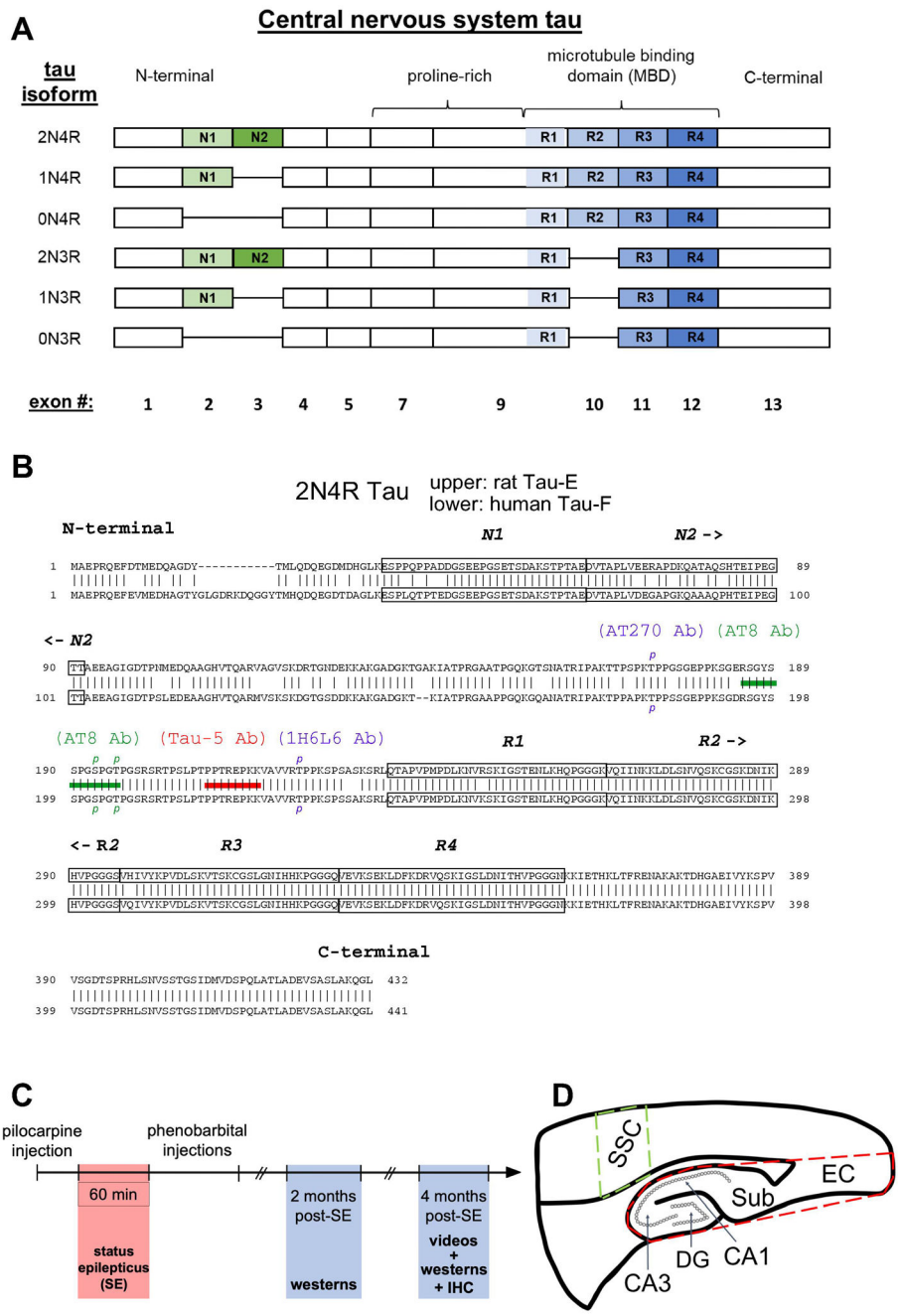

Figure 1.

Tau isoform composition. **(A)** Schematics of the six tau isoforms formed by alternative splicing of N-terminal exons (*N1*, *N2*, *green-shaded*) and of repeat domains (*R1-R4*, *blue-shaded*) within the microtubule binding region (*MBD*). The presence of none, one, or two N-terminal exons determines 0N, 1N, 2N tau isoform specificity, correspondingly; while the absence or presence of the R2 domain within the MBD generates 3R or 4R tau isoforms, respectively. Labeling at bottom is the exon number of the human microtubule associated protein tau gene, *MAPT*, that encodes for the corresponding domain above. Exons 6 and 8 are not expressed in the central nervous system. **(B)** Comparison of 2N4R tau amino

acid sequences between rat *(upper)* and human *(lower)* showing 89% homology between the two species. Tau naming for each species found in Uniprot.org. The two N-terminal exons and four repeat domains are boxed within the sequences. Shown are epitopes for anti-tau antibodies (Abs) Tau-5 Ab *(red bar)* and AT8 Ab *(green bar)*. To be recognized by the AT8 Ab, both S193 and T196 rat tau residues (S202 and T205 in humans) must be phosphorylated, denoted by *green p*'s. Additionally, two other phosphorylated tau residues, T172 rat/T181 human recognized by the AT270 Ab and T222 rat/T231 human recognized by the 1H6L6 Ab, are labelled as *blue p*'s. **(C)** Timeline of experiments involving the pilocarpine-induced rat model of chronic epilepsy. **(D)** Schematic of brain regions studied. Whole hippocampal formation encompassing *CA1* and *CA3* hippocampus, dentate gyrus (*DG*), subiculum (*Sub*), and entorhinal cortex (*EC*) is enclosed within the *dashed red border*. A region within the somatosensory cortex (*SSC*, *dashed green boundary)* served as control tissue outside the putative seizure onset zone within the hippocampus.

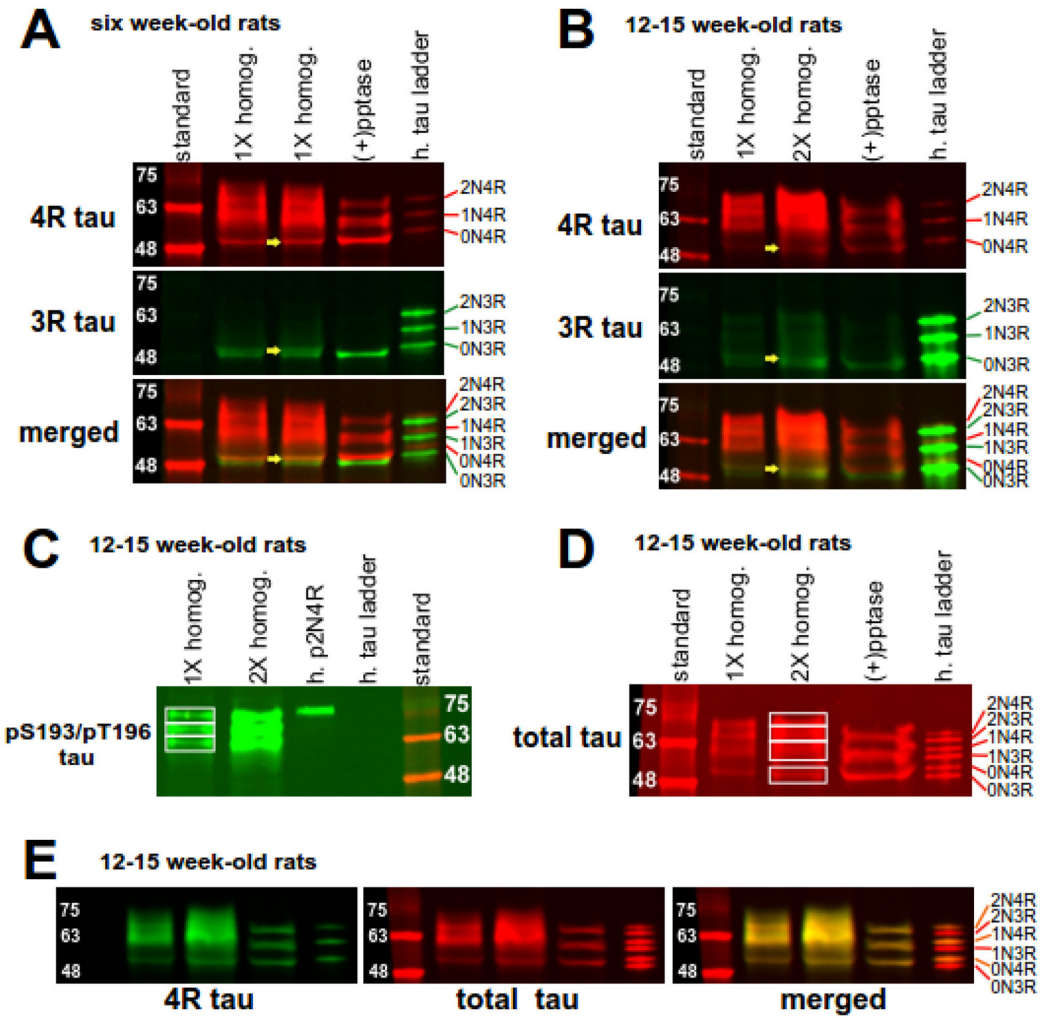

Figure 2.

Expression of tau isoforms in hippocampal tissue. A ladder containing six human tau isoforms (*h. tau ladder*) allows for size comparison and serves as a negative control for phosphorylation. **(A)** 4R and 3R tau expression in raw tissue homogenate either without *(1X homog.)* or with phosphatase treatment [*(+) pptase*] from six week-old naïve rats. In the raw homogenate lanes of the *top panel* displaying 4R tau isoforms, tau proteins migrate between 50 to 72 kDa. Consolidation of these isoforms into three protein bands in phosphatase-treated homogenates indicate 4R tau isoforms are highly phosphorylated. In the raw homogenate lanes displaying 3R tau (*middle panel*), a doublet around 50 kDa converged into the lower band after phosphatase treatment. The *bottom panel* is a merged image showing four main tau isoforms. The *yellow arrows* in the three panels demonstrate that the upper doublet band in the merged panel consists of 0N3R tau and 0N4R tau. **(B)** 4R and 3R tau expression in 12-15 week-old naïve rats. Tau expression is similar as above, except for notably decreased expression of both 0N3R and 0N4R isoforms in the older rats. **(C)** AT8 Ab staining of dually phosphorylated S193/T196 tau in brain homogenates from 12-15 week old rats. Three tau bands are observed. Phosphorylated 2N4R human tau (*h. p2N4R*) served as a positive control for detection of dually phosphorylated S193/T196 tau.

(D) Total tau staining of rat brain homogenates with the Tau-5 Ab. Four bands of staining are observed in raw homogenates. Phosphatase treatment consolidates staining to three bands. **(E)** Complete overlapping (*merged*) of bands composed of 4R tau (*4R tau, green*) and total tau (*total tau, red*) demonstrates that total tau staining reflects 4R tau expression in brain homogenates of 12-15 week-old rats.

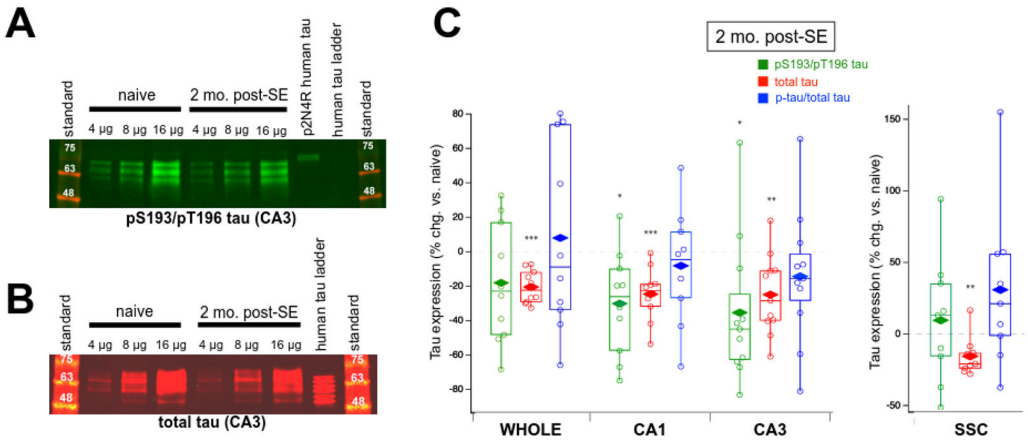

Figure 3.

Dual pS193/pT196 tau and total tau expression in brain tissue of two month post-SE rats. **(A)** Representative western blot of phosphorylated tau expression in CA3 hippocampal region using the AT8 Ab showing a decrease in phosphorylated tau expression in chronic epilepsy. Shown are three different loading amounts for naïve and epileptic conditions. Phosphorylated p2N4R human tau and human tau ladder served as positive and negative controls, respectively, for the detection of phosphorylated tau. **(B)** Representative western blot of total tau expression in rat CA3 hippocampus using the Tau-5 Ab demonstrating a modest reduction in total tau expression in chronic epilepsy. The human tau ladder provided a size reference. **(C)** Group data showing changes in tau expression in chronically epileptic rats at two months post-SE in the whole hippocampal formation, CA1 hippocampus, CA3 hippocampus, and somatosensory cortex (SSC) compared to age-matched naïve rats. Values shown are individual data points; boxes denoting median, 75th and 25th percentiles; whiskers showing 95th and 5th percentiles; and mean value (*diamonds*). Only the CA1 and CA3 hippocampal regions of chronically epileptic rats showed significantly reduced dual pS193/pT196 tau (*green box plots*). Reductions in total tau expression were found in every region, including the SSC (*red box plots*). No changes were observed in fractional dually phosphorylated tau (pS193/pT196 tau/total tau) in any region (*blue box plots*).

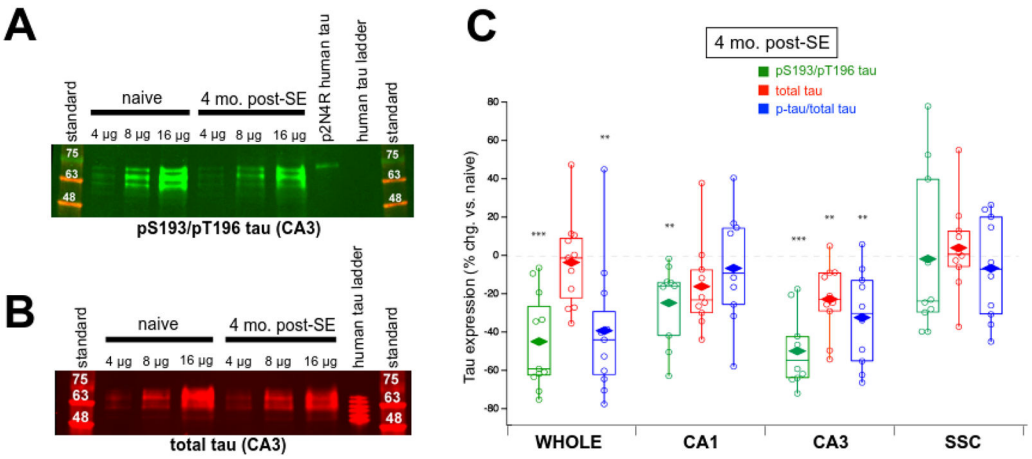

Figure 4.

Dual pS193/pT196 tau and total tau expression in brain tissue of four month post-SE rats. **(A)** Representative western blot showing greatly decreased dual pS193/pT196 tau expression in CA3 hippocampus in chronic epilepsy using the AT8 Ab. **(B)** Representative western blot demonstrating a modest reduction in total tau expression in CA3 hippocampal regions using the Tau-5 Ab in chronic epilepsy. **(C)** Group data showing changes in tau expression in chronically epileptic rats at four months post-SE in the whole hippocampal formation, CA1 hippocampus, CA3 hippocampus, and somatosensory cortex (SSC) compared to age-matched naïve rats. Values shown are individual data points; boxes denoting median, 75th and 25th percentiles; whiskers showing 95th and 5th percentiles; and mean value (*diamonds*). Significant decreases in dual pS193/pT196 tau were observed in all hippocampal regions in epilepsy (*green box plots*). The only change in total tau expression was the decrease observed in the CA3 hippocampus (*red box plots*). Reductions in fractional pS193/pT196 tau expression (pS193/pT196 tau/total tau) were detected in the whole hippocampal formation and in the CA3 hippocampus (*blue box plots*). No change in tau expression was seen in the SSC.

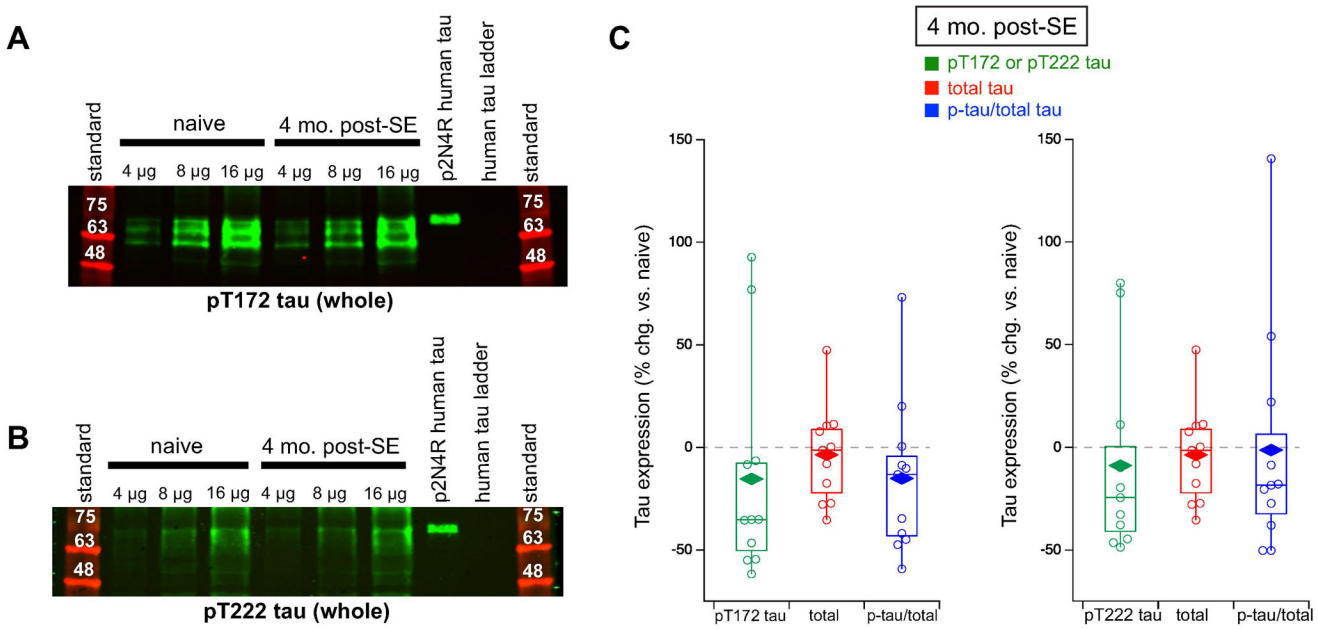

Figure 5.

pT172tau, pT222 tau, total tau expression, and fractional phosphorylated tau in whole hippocampal formation from four month post-SE rats. **(A)** Representative western blot showing unchanged pT172 tau expression in the whole hippocampal formation in chronic epilepsy using the AT270 Ab. **(B)** Representative western blot showing unchanged pT222 expression in the whole hippocampal formation in chronic epilepsy using the 1H6L6 Ab. **(C)** Group data showing no changes in either pT172 tau expression (*left*) or pT222 tau expression (*right*) in chronically epileptic rats. Data for total tau expression is the same as total tau expression in whole hippocampal formation used in Figure 4.

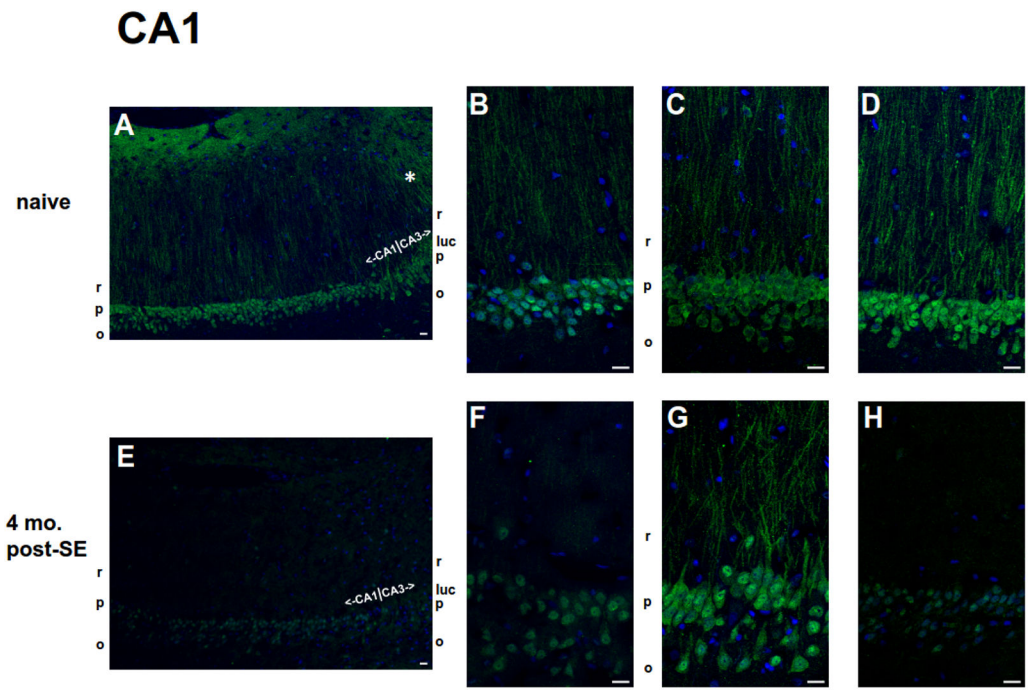

Figure 6.

Localization of pS193/pT196 tau protein in the hippocampal CA1 region within age-matched naïve **(A-D)** and chronic 4 mo. post-SE **(E-H)** rats by AT8 Ab staining. pS193/pT196 tau staining is shown in *green*, and nuclear staining by 4′,6-diamidino-2-phenylindole (DAPI) is shown in *blue*. Scale bars = 20 μm. **(A-D)** The lower magnification image (A) represents a larger scale view of pS193/pT196 tau staining within the CA1 hippocampus of naïve rats. The boundary between CA1 and CA3 hippocampal subregions is demarcated. Note the qualitative increased dendritic staining within the CA3 hippocampus (*) compared to that within the CA1 hippocampus at the transition. pS193/pT196 tau staining examples from three different naïve rats of a magnified view within the CA1 subregion are displayed in (B-D). The most abundant expression of pS193/pT196 tau was observed in the CA1 somata within the stratum pyramidale (*p*) layer; some staining was present in the dendrites in the stratum radiatum layer (*r*), while little to no staining was observed in the axons within the stratum oriens (*o*). **(E-F)** The lower magnification image (E) represents a larger scale view of pS193/pT196 tau staining within the CA1 hippocampus of 4 mo. post-SE of chronically epileptic rats with the boundary between the CA1 and CA3 hippocampal subregions labelled. pS193/pT196 tau staining examples from three different chronically epileptic rats of a magnified view within the CA1 subregion are displayed in (F-H). The distribution of pS193/pT196 tau within the CA1 hippocampus in chronically epileptic rats was similar to that in age-matched naïve rats: the greatest expression was observed within the stratum pyramidale (*p*) layer; lesser extent in the stratum radiatum layer (*r*), while little to no staining within the stratum oriens (*o*). Overall, pS193/pT196 tau staining in the CA1 hippocampal subregion of chronically epileptic rats qualitatively was less than that of naïve rats.

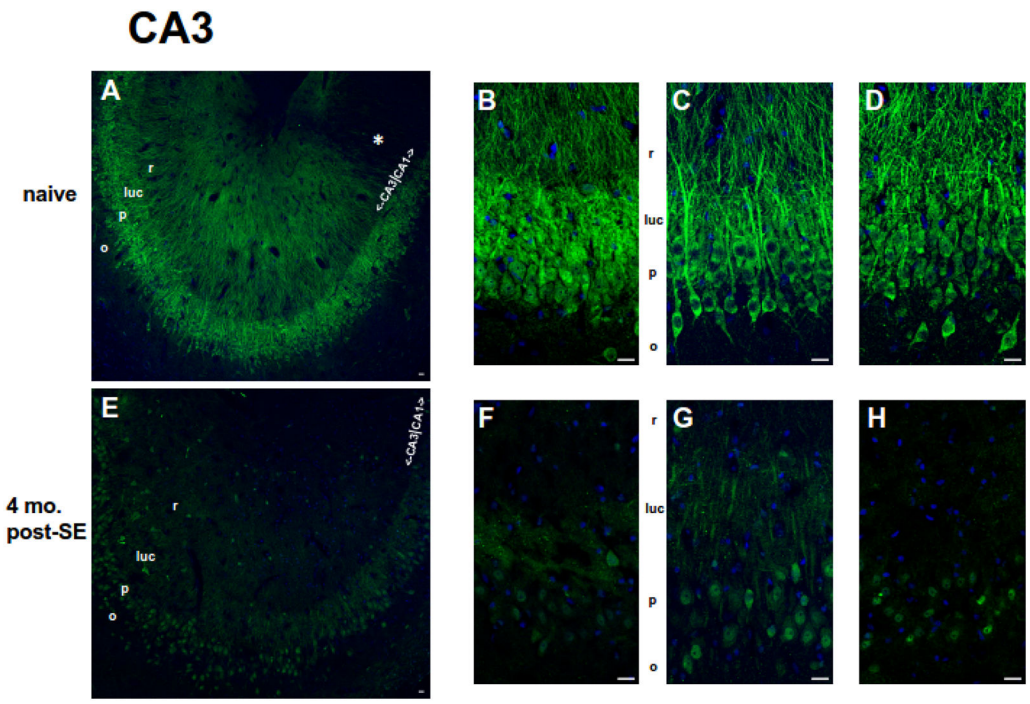

Figure 7.

Localization of pS193/pT196 tau protein in the hippocampal CA3 region within age-matched naïve **(A-D)** and chronic 4 mo. post-SE **(E-H)** rats by AT8 Ab staining. pS193/pT196 tau staining is shown in *green*, and DAPI is shown in *blue*. Scale bars = 20 μm. **(A-D)** The lower magnification image (A) represents a larger scale view of pS193/pT196 tau staining within the CA3 hippocampus of naïve rats. The boundary between CA1 and CA3 hippocampal subregions is included. Note the qualitative decreased dendritic staining within the CA1 hippocampus (*) compared to that within the CA3 hippocampus at the transition. pS193/pT196 tau staining examples from three different naïve rats of a magnified view within the CA3 subregion are displayed in (B-D). The most abundant region of dually phosphorylated S193/T196 tau expression was observed in the axons of mossy fibers within the stratum lucidum layer (*luc*) and in the cell bodies within the stratum pyramidale (*p*) layer. Less staining was observed in the dendrites originating from the stratum radiatum layer (*r*). Like the CA1 hippocampus, pS193/pT196 tau staining was lowest in the axons within the stratum oriens (*o*) layer. **(E-F)** The lower magnification image (E) represents a larger scale view of pS193/pT196 tau staining within the CA3 hippocampus of chronically epileptic rats. The boundary between the CA1 and CA3 hippocampal subregions is noted. pS193/pT196 tau staining examples from three different chronic rats of a magnified view within the CA3 subregion are displayed in (F-H). The distribution of pS193/pT196 tau within the CA3 hippocampus in chronically epileptic rats was similar to that in age-matched naïve rats: the greatest expression was observed in the stratum lucidum layer (*luc*) and within the stratum pyramidale (*p*) layer; lesser extent in the stratum radiatum layer (*r*), while little to no staining within the stratum oriens (*o*). Overall, pS193/pT196 tau staining qualitatively was reduced throughout the CA3 hippocampal subregion in chronically epileptic rats compared to that in naïve rats.